Two-Dimensional Simulation of Electrothermal Deicing of Aircraft Components

W. B. Wright,* T. G. Keith Jr.,† and K. J. De Witt‡
University of Toledo, Toledo, Ohio

The transient, two-dimensional heat transfer occurring in an electrothermal deicer pad was simulated using a number of finite-difference numerical methods. The alternating direction implicit method was found to be the most efficient procedure for this problem. A parametric study was performed to investigate the effects of gap width, nodal spacing, variable ice thickness, and variable outer heat-transfer coefficient on the solution. The results show that a two-dimensional simulation is required when the ratio of the heater length to the gap length is less than 2.5. To predict ice-interface temperature and melt times, the surface heat-transfer coefficient variation does not have to be considered except when the ice is very thin. In addition, for a heater wattage of 30 W/in.^{2}, a nonuniform ice thickness can be modeled as a constant thickness if the ice is at least 0.125 in. thick at every location. A comparison of the numerical results with experimental data shows good agreement and serves to benchmark the code.

Nomenclature

C_p = specific heat capacity, Btu/lb-°F
d = ice thickness, in.
H = enthalpy, Btu/ft^3
h = heat-transfer coefficient, Btu/h-ft^2-°F
k = thermal conductivity, Btu/hr-ft-°F
L_f = latent heat of fusion for ice, Btu/lb
q = rate of heat generation per unit volume, W/in.^{3}
T = temperature, °F
t = time variable, h
x = space coordinate in x direction, in.
y = space coordinate in y direction, in.
α = thermal diffusivity, ft^2/h
ρ = density, lb/ft^3

Subscripts

1 = liquid
lm = liquid at the melting point
m = melting point
s = solid
sm = solid at the melting point

Introduction

THE removal and/or prevention of ice on aircraft components, e.g., wing surfaces, nacelles, inlets, and so forth, is vital to aircraft performance and operation. Even small amounts of ice can have disastrous consequences. Methods of ice control can be divided into two broad categories: anti-icing methods and deicing methods. Anti-icing methods are concerned with the prevention or minimization of ice buildup on aircraft surfaces. These methods generally involve chemical or thermal principles. Deicing methods are concerned with ice removal after and during ice buildup; they are generally based on mechanical or thermal principles.

Presented as Paper 88-0288 at the AIAA 26th Aerospace Sciences Meeting Reno, NV, Jan. 11–14, 1988; received April 27, 1988; revision received Dec. 7, 1988.

*Graduate Assistant, Department of Chemical Engineering.
†Professor, Department of Mechanical Engineering.
‡Professor, Department of Chemical Engineering.

An electrothermal deicer pad is a widely used thermal deicing system. By this method of ice control, heater pads are installed beneath the skin of a wing surface surrounding the leading edge, as shown in Fig. 1. The heaters are activated during icing conditions to remove accreted ice. Electrical energy in the form of conducted heat destroys the adhesion forces at the ice-surface. Aerodynamic forces then readily sweep the ice from the surface.

A two-dimensional representation of a deicer pad in a rectangular coordinate system is illustrated in Fig. 2. The pad consists of five layers: a substrate (blade) layer; an insulation layer below the heater; a resistance heater; a thinner insulation layer above the heater so that the majority of the energy moves upward; and an abrasion shield to protect the heater. On top of the abrasion shield is an ice layer. This model represents one section of the blade which has a heater and a gap between heaters. The insulated boundaries comprise lines of symmetry, indicating that the heater-gap sequence continues throughout the blade. The heat-transfer coefficient on the bottom, h_1, represents free convection, whereas the top coefficient, h, is for forced convection.

A variety of numerical models have been developed to simulate deicer pad performance. The first was by Stallabrass,[1] who developed both one- and two-dimensional computer models. Baliga,[2] Marano,[3] Gent and Cansdale,[4] and Roelke[5] all developed one-dimensional models (no heater gaps) using separate numerical techniques. Chao[6] developed a two-dimensional model that was later revised by Leffel.[7] Wright[8] considered a more complex two-dimensional problem than either Chao or Leffel and compared several solution methods. Masiulaniec[9] developed a body-fitted coordinate system in order to model the true blade shape. All of these investigations were designed to model the phase change of the ice layer and to predict transient temperature distributions in composite layers.

Analysis

The transient temperature distribution in a layered body containing heat sources is described by

$$\rho_j C_{p_j} \frac{\partial T_j}{\partial t} = k_j \frac{\partial^2 T_j}{\partial x^2} + k_j \frac{\partial^2 T_j}{\partial y^2} + q_j \tag{1}$$

where j designates the layer number and q_j is the rate of heat generation per unit volume and is nonzero only for the heater layer. For a multilayered body, the solution of Eq. (1) is

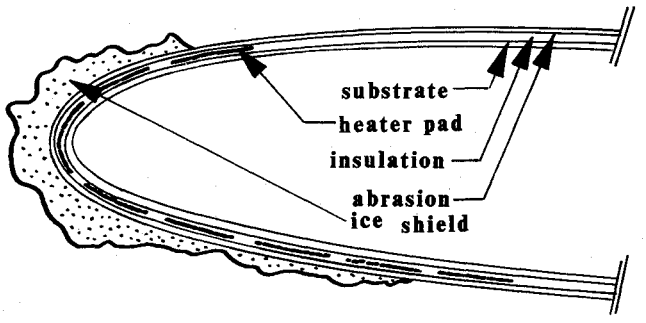

Fig. 1 Airfoil with electrothermal deicer pad.

impractical by any means other than numerical calculation. In this work, only finite-difference methods have been considered.

The finite-difference method discretizes the continuous time and space domains into a grid of nodes. A system of algebraic equations based on this grid replaces the governing differential equations and boundary conditions. This system of equations can be solved to determine the instantaneous value of the dependent variable at a particular node in the grid. Accuracy of finite-difference methods depends on the particular discretization method used and the grid spacing. For example, a simple explicit method is first-order accurate in time and second-order accurate in space, whereas a Crank-Nicolson scheme is second-order accurate in both time and space.

Many finite-difference schemes can be found in the literature. Several of these have been applied to deicer modeling. Stallabrass[1] and Gent and Cansdale [4] both used an explicit method with forward-time, central-space differencing. Roelke[5] used a purely implicit method with forward-time, central-space differencing. Baliga,[2] Marano,[3] Chao,[6] and Leffel[7] used the Crank-Nicolson scheme, which is an implicit scheme that has central-time and central-space differencing. Implicit methods have been used to eliminate stability requirements of explicit methods.

After finite-differencing the differential equations, a variety of numerical techniques can be used to solve the corresponding matrix system of algebraic equations. The technique used may be determined by the finite-differencing method, however. For example, the simple explicit scheme needs no solution technique as all new temperatures are directly calculated from previously known values. For the two-dimensional heat conduction equation, this method requires that the time step (Δt) be less than $[(\Delta x)^2 + (\Delta y)^2]/2\alpha$ to insure stability, where α is the thermal diffusivity and Δx and Δy are the space increments.

On the other hand, the Crank-Nicolson scheme is implicit and, therefore, is often solved using an iterative solution technique. Baliga[2] used Gaussian elimination to solve for the temperatures. However, this procedure is very time-consuming for a two-dimensional problem. Marano,[3] Chao,[6] and Leffel[7] used Gauss-Seidel iteration instead. Moreover, the abrupt change in enthalpy at the melt temperature in the phase-change procedure employed dictated that an iterative procedure be used.

Recently, Wright[8] investigated nine numerical schemes in order to determine which was the most efficient for modeling deicer pad designs. These methods were selected from those described by Anderson et al.[10] Three of these, the simple explicit, the Crank-Nicolson, and the simple implicit methods, have been used by previous investigators. The other six are the Hopscotch, ADE (alternating direction explicit), ADI (alternating direction implicit), time splitting (the method of fractional steps), SIP (strongly implicit procedure), and MSIP (modified strongly implicit procedure). It was found that the ADI method was the most efficient procedure for this problem. It was approximately twice as fast as its nearest competitor, MSIP, and was up to 25 times faster than the Crank-Nicolson formulation used by Chao[6] and Leffel.[7] ADI is faster than the other methods for two main reasons. First, ADI employs a direct solution method and therefore iteration is not required. Second, the time step necessary to obtain an accurate solution with this method is larger than that needed for the explicit methods considered here.

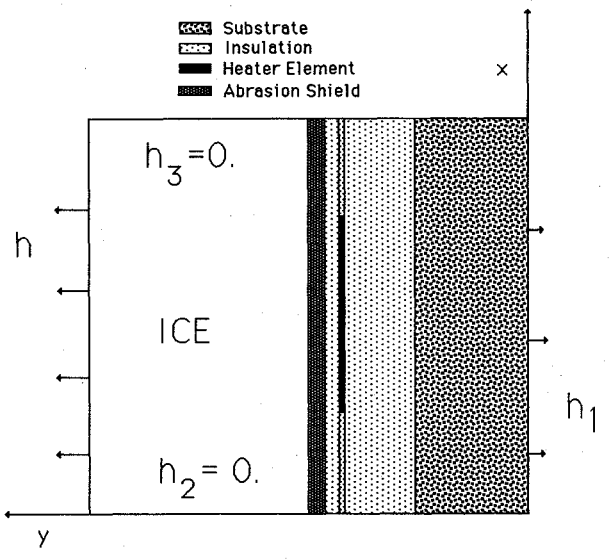

Fig. 2 Standard deicer pad.

In order to simulate an electrothermal deicer pad completely, the melting of accreted ice must be modeled. Stallabrass[1] modeled the phase change by simply holding a node at the melting point until sufficient energy had accumulated to completely melt the node. Baliga[2] used a formulation proposed by Bonacina et al.[11] that associates the latent heat effect with a finite temperature interval about the phase-change isotherm. The other models previously mentioned all used a technique described by Voller and Cross[12] and Voller et al.[13] known as the enthalpy method. The enthalpy method is also termed a weak solution method because it is based on an integral formulation. In this procedure, temperature is calculated from enthalpy and is therefore not calculated directly.

The enthalpy method uses the conservation of energy equation formulated in terms of two dependent variables, temperature and enthalpy:

$$\frac{\partial H_{\text{ice}}}{\partial t} = \frac{\partial}{\partial x}\left(k_{\text{ice}}\frac{\partial T_{\text{ice}}}{\partial x}\right) + \frac{\partial}{\partial y}\left(k_{\text{ice}}\frac{\partial T_{\text{ice}}}{\partial y}\right) \tag{2}$$

The enthalpy within both phases (ice and water) can be found from Eq. (2). The temperature can then be determined from the following relation between H and T:

$$H = \begin{cases} \rho_s C_{ps} T & T < T_m \\ \rho_l C_{pl}(T - T_m) + \rho_l(C_{ps} T_m + L_f) & T > T_m \end{cases} \tag{3}$$

Inverting gives

$$T = \begin{cases} H/\rho_s C_{ps} & H < H_{sm} \\ T_m & H_{sm} < H < H_{lm} \\ (H - H_{lm})/\rho_l C_{pl} + T_m & H > H_{lm} \end{cases} \tag{4}$$

with

$$H_{sm} = \rho_s C_{ps} T_m \tag{5a}$$

$$H_{lm} = \rho_l(C_{ps} T_m + L_f) \tag{5b}$$

Predicting the location of the solid-liquid interface is not required because this is determined by nodal enthalpy alone. The temperature at any point is then calculated using the known enthalpy-temperature relationship. The equivalence of this method and the classical formulation of the ablation problem was proven by Atthey.[14] The previous investigations that used the enthalpy method accounted for the abrupt change in enthalpy that occurs during melting at a constant melt temperature of 32°F. This non-one-to-one relationship between enthalpy and temperature required that an iterative solution procedure be used in order to find the appropriate temperature at each point. Roelke[5] and Wright[8] altered the enthalpy method by the use of a small temperature interval at the melting point, which is similar to the method used by Baliga.[2] This adjustment was made to take advantage of a recent technique proposed by Schneider and Raw[15] to predict temperatures during phase change in a more expedient fashion. Their technique assumes the phase at each point in the ice so that the enthalpy can be eliminated in favor of temperature prior to calculation. This, in turn, permits the use of noniterative solution methods that allow the new temperature at each point to be determined more efficiently than by the use of iterative methods. The assumed phase of each mode is then updated as the solution proceeds. This technique, which will be termed the method of assumed states, has been used by Roelke[5] in a one-dimensional deicer pad analysis and by Wright[8] in a two-dimensional analysis.

Over the past few years, various computer codes related to this problem have been developed at the University of Toledo. These codes, along with some of their capabilities, are listed in Table 1.

Discussion of Numerical Results

In the previous section, finite-difference numerical methods have been briefly discussed, all of which are capable of solving the equations describing the transient two-dimensional heat transfer in an electrothermal deicer pad. The codes developed from these methods will now be evaluated to determine the conditions for which one-dimensional codes are sufficient for deicing analysis, or for which two-dimensional procedures are necessary. Since a one-dimensional simulation will obtain results in significantly less computational time than required by a two-dimensional simulation, this analysis will be valuable. A comparison will be made with experimental data obtained by Leffel.[7] This comparison illustrates the validity of the computer models discussed previously.

Parameter Variation

In this section, a parametric study of some of the key variables of the problem will be performed in order to determine their effect on the solution. Since a multitude of variables could be studied, this discussion will focus on those variables that are responsible for making the problem two-dimensional. These variables are chosen so that a determination can be made as to when the two-dimensional nature of the problem disallows use of a one-dimensional simulation. If a one-dimensional model is adequate for a particular problem, the use of a one-dimensional code such as those developed by Marano[3] or Roelke[5] will greatly decrease the amount of computer time needed to solve the problem. Using the current approach, i.e., the ADI method, the difference in computation times between one- and two-dimensional models has been greatly reduced, but it is still significant for a reasonably complex problem.

There are four variables that reflect the two-dimensional nature of the problem. First and foremost is the size of the heater gap and the physical properties of the gap. Second is the grid spacing used. A determination of the number of nodes necessary for solution is also necessary for the purpose of determining an accurate solution. Third, a variable ice shape

Table 1 Summary of computer codes

Methods used		Capabilities
One-dimensional		
Baliga[2]	High heat capacity Crank-Nicolson Gauss elimination	Variable Δy in each layer Variable heater cycling times Selectable ice growth rates
Marano[3]	Enthalpy method Crank-Nicolson Gauss-Seidel iteration	
Roelke[5]	Method of assumed states Cubic splines technique Tridiagonal matrix algorithm	
Two-dimensional rectangular		
Chao[6]	Enthalpy method Crank-Nicolson Gauss-Seidel iteration	Single heater Variable grid in y direction Variable heater cycling times Heater conductivities used in gap
Leffel[7]	Enthalpy method Crank-Nicolson Gauss-Seidel iteration	Leffel code has variable ice shape
Wright[8]	Method of assumed states Several numerical methods (ADI best), ADI uses tridiagional matrix algorithm	Multiple heaters Variable grid in both directions Variable heater cycling times Variable ice shape and growth rates Variable outer heat-transfer coefficient
Two-dimensional body-fitted		
Masiulaniec[9]	Enthalpy method Crank-Nicolson Gauss-Seidel iteration	Same as Wright, plus coordinates are changed to fit the shape of the body

can significantly alter the temperature profiles, especially if there are regions on the blade that have no ice. Finally, a variable outer ambient heat-transfer coefficient can have an impact on the dimensionality of the problem.

Gap Size and Material

The size of the heater gap is the primary factor in determining whether two-dimensional effects are important in a deicer pad. The material in the heater gap is also critical since this can drastically alter the temperature of the heater. For simplicity, Chao[6] used the same material in the gap as was present in the heater. The current analysis will show when this is not a good approximation.

A standard deicer is simulated with a power density of 30 W/in.^{2} for 20 s of real time. The width of the heater is kept at 0.25 in. and the gap width is varied from 0.05 to 0.50 in. in increments of 0.05 in. The ambient temperature is 10°F, and the inner and outer heat-transfer coefficients h_1 and h are 1 and 150 Btu/h-ft^2-°F, respectively. Table 2 presents physical properties and typical parameters for a standard deicer pad.

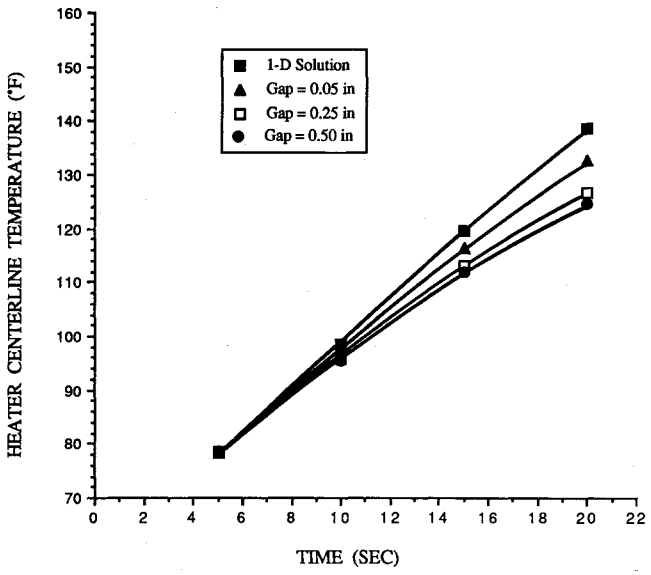

Fig. 3 Variation in heater centerline temperature with gap size ($k_{gap} = k_{insulation}$).

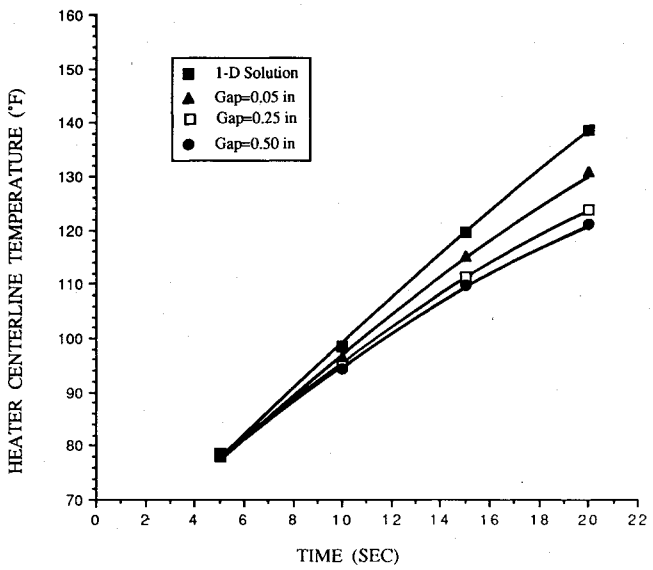

Fig. 4 Variation in heater centerline temperature with gap size ($k_{gap} = k_{heater}$).

Figure 3 presents the temperature vs time at the centerline of the heater for the case when the physical properties of the gap are the same as those for the surrounding insulation. The same cases were run using the properties of the heater in the gap and are shown in Fig. 4. As can be seen, significant deviation from the one-dimensional result (zero gap thickness) is apparent even at small gap thicknesses. This deviation is larger for the second cases that use the same conductivity in the gap than for the cases using a lower conductivity. These two cases are compared directly in Fig. 5, which plots heater temperature after 20 s of simulated time vs gap thickness for both sets of cases considered.

A similar set of plots are made that plot gap centerline temperature instead of heater centerline temperature for the same two sets of cases described previously. These plots, Figs. 6–8, show an even greater dependence on the gap size, as well as a greater dependence on the properties used in the gap. The reason that gap temperatures are significant is that it may be necessary for the entire bottom layer of the ice to melt for the adhesion of the ice to the metal abrasion shield to be broken. Once this adhesion is broken, dynamic forces will remove the ice from the surface. If the gap temperatures are severely affected by the size of the gap, it will take longer to remove the ice from the surface because the temperatures at the ice-abrasion shield interface will be likewise affected.

A two-dimensional analysis is needed to model accurately the problem when the ratio of the heater length to the gap length is less than 2.5. For heater-to-gap ratios larger than this, it is felt that the decrease in heater and gap temperatures is not large enough to seriously affect the rate of ice removal. For ratios smaller than this, the combination of increasing gap size and, thus, increased ice adhesion to the surface and decreased temperatures at the surface make the use of a two-di-

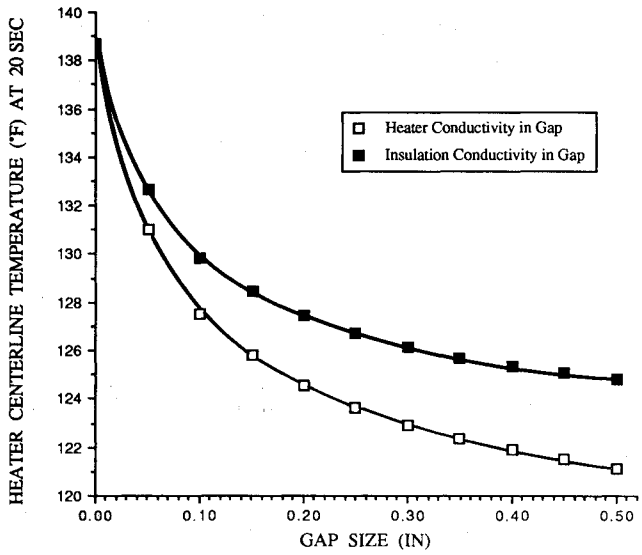

Fig. 5 Effect of gap conductivity on heater centerline temperature.

Table 2 Physical properties of a standard deicer pad

Layer	Thickness, in.	Thermal conductivity, Btu/h-ft^2-°F	Thermal diffusivity, ft^2/h
Ice	0.250	1.29	0.0446
Stainless steel abrasion shield	0.012	8.70	0.1500
Epoxy/glass insulation	0.010	0.22	0.0087
Heater element	0.004	7.60	0.1380
Epoxy/glass insulation	0.050	0.22	0.0087
Aluminum substrate	0.087	66.50	1.6500

Table 3 Data for experimental deicer pad

Layer	Thickness, in.	Thermal conductivity, Btu/h-ft-°F	Thermal diffusivity, ft^2/h
Stainless steel abrasion shield	0.0300	8.70	0.1500
Epoxy adhesive	0.0168	0.10	0.0058
Epoxy/glass insulation	0.0138	0.22	0.0087
Epoxy adhesive	0.0082	0.10	0.0058
Copper heater element	0.0065	60.00	1.1500
Epoxy adhesive	0.0082	0.10	0.0058
Epoxy/glass insulation	0.0138	0.22	0.0087
Epoxy adhesive	0.0082	0.10	0.0058
Stainless steel blade skin	0.0200	8.70	0.1500
Epoxy adhesive	0.0100	0.10	0.0058
Aluminum doubler	0.0500	102.00	2.8300
Epoxy adhesive	0.0100	0.10	0.0058
Aluminum substrate	0.1750	102.00	2.8300

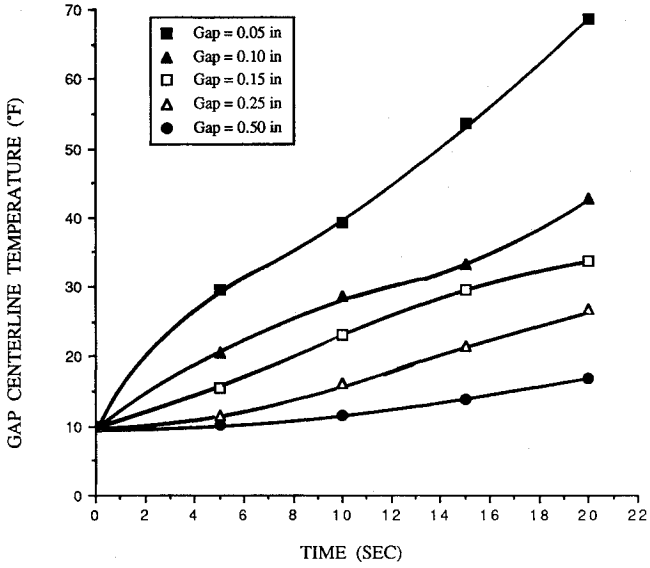

Fig. 6 Variation in gap centerline temperature with gap size ($k_{gap} = k_{insulation}$).

mensional model necessary. Furthermore, the gap properties should always be modeled using the physical properties of the surrounding insulation, as the use of different properties in the gap has been shown to be a significant parameter in determining heater temperatures.

Grid Spacing

The number of nodes in both the heater and the gap were varied to study what effect, if any, this had on the results. The same cases that were used for determining the effect of gap size were run using from 3 to 20 nodes in the heater, and from 1 to 20 nodes in the gap. For all of the cases studied, 6 nodes were found to be the minimum necessary in the heater in the x direction, regardless of its size. Four nodes were the minimum necessary in the gap for large gap sizes (heater length/ gap length < 1), but as few as 2 nodes could be used in the gap for small gap sizes (heater length/ gap length > 5).

It was found that the grid spacing in the heater in the y direction should be at least an order of magnitude smaller than it is in the x direction. This is especially true for large heater-to-gap ratios. This is understandable since the majority of the heat flow is in the y direction and the largest temperature gradients will be found in the y direction. A finer grid in regions that have temperature gradients is necessary to insure an accurate solution.

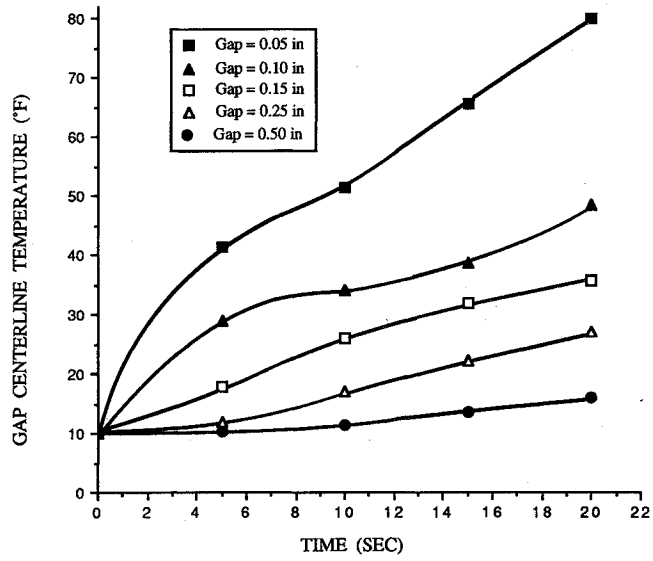

Fig. 7 Variation in gap centerline temperature with gap size ($k_{gap} = k_{heater}$).

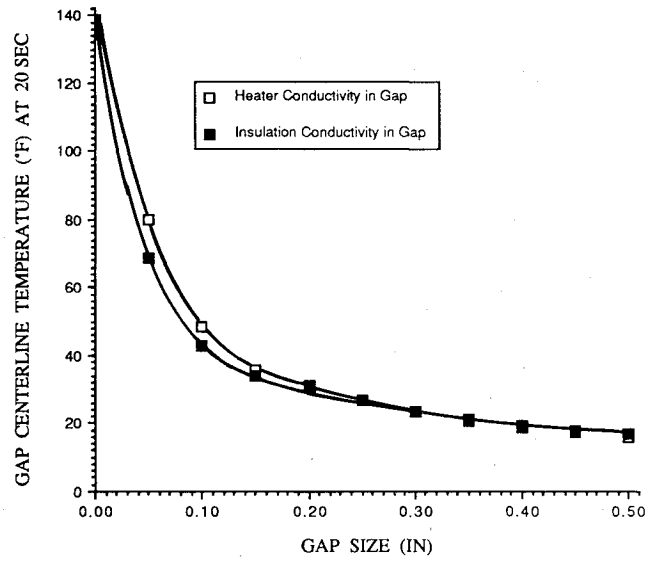

Fig. 8 Effect of gap conductivity on gap centerline temperature.

Ice Thickness and Heat-Transfer Coefficient

The thickness of the ice layer and the outer heat-transfer coefficient can have a significant effect on the temperature profiles in the deicer pad, especially on the temperature at the interface between the pad and the ice. The same standard deicer case as described previously was run using various ice thicknesses and outer heat-transfer coefficients in order to determine at what point, if any, these parameters cease to have an impact to the results. This becomes especially important in modeling cases that have variable ice shapes and variable heat-transfer coefficients. It is important to determine how precisely each of these parameters needs to be measured. These cases, however, do not contain a gap in the heater layer so that the effect of these parameters on the solution could be distinguished from the effect of the gap size on the solution.

Figure 9 shows a plot of temperature vs time at the ice-abrasion shield interface for four different ice thicknesses d and four different outer heat-transfer coefficients h for a total of 16 cases. The four ice thicknesses used were 0.03125, 0.0625, 0.125, and 0.25 in. The four heat-transfer coefficients used were 40, 80, 120, and 160 Btu/h-ft^2-°F. As can be seen, the ice-interface temperature decreases slightly when the ice thick-

ness increases for a constant heat-transfer coefficient. For the same ice thickness, an increase in the heat-transfer coefficient decreases the interface temperature. For ice thicknesses greater than 0.125 in., the heat-transfer coefficient has no effect on the interface temperature as a function of time. In essence, Fig. 9 is a one-dimensional result.

Variable ice thickness cases and variable heat-transfer coefficient cases were also run with the standard deicer described previously. Figure 10 shows the variation in the ice-abrasion shield interface temperature after 20 s as a function of ice thickness for heat-transfer coefficients of 40, 80, 120, and 160 Btu/h-ft^2-°F, where these heat-transfer coefficients are constant for that particular run, but ice thickness is a function of the x position. For an ice thickness of 0.05 in., the ice interface temperature after 20 s decreases from 52.7 to 43.4°F as the heat-transfer coefficient changes form 40 to 160 Btu/h-ft^2-°F. Approximately the same variation occurs at other ice thicknesses. The two-dimensionality of the problem is evident from the difference in temperature magnitude shown by the curves.

Figure 11 shows a similar plot, but presents the ice-abrasion shield interface temperature after 20 s as a function of heat-transfer coefficient for constant ice thicknesses of 0.0625, 0.125, and 0.25 in. In this plot, the outer heat-transfer coefficient is a function of the x position. Again, the two-dimensionality of the problem is shown by the different temperature levels. For a heat-transfer coefficient of 40 Btu/h-ft^2-°F, the ice interface temperature after 20 s drops from 52.7 to 47 °F as the ice thickness increases from 0.0625 to 0.25 in. At a constant ice thickness, very slight interfacial temperature variation is seen as the heat-transfer coefficient increases for ice thicknesses greater than 0.125 in.

Figures 10 and 11 show that the ice-abrasion shield interface temperature depends on both the ice thickness and the heat-transfer coefficient when both are varying with position. However, the temperature change due to a variable ice shape is larger than that due to a variable heat-transfer coefficient.

Figure 12 shows a plot of melt time vs ice thickness for the four heat-transfer coefficients used in these cases, and Fig. 13 shows melt time vs heat-transfer coefficient for the four ice thicknesses run. The same points are being plotted in these two figures, but are plotted in two different ways for comparative purposes. Melt time is defined as the time needed for the

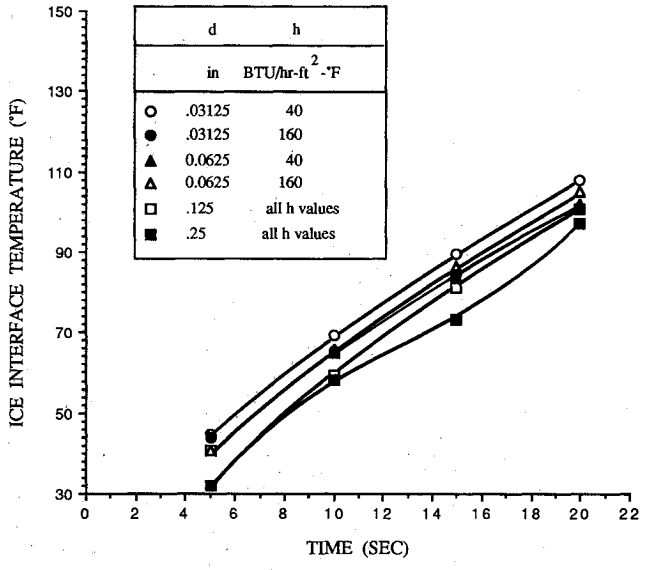

Fig. 9 Effect of ice thickness and outer heat-transfer coefficient on ice-abrasion shield interface temperature.

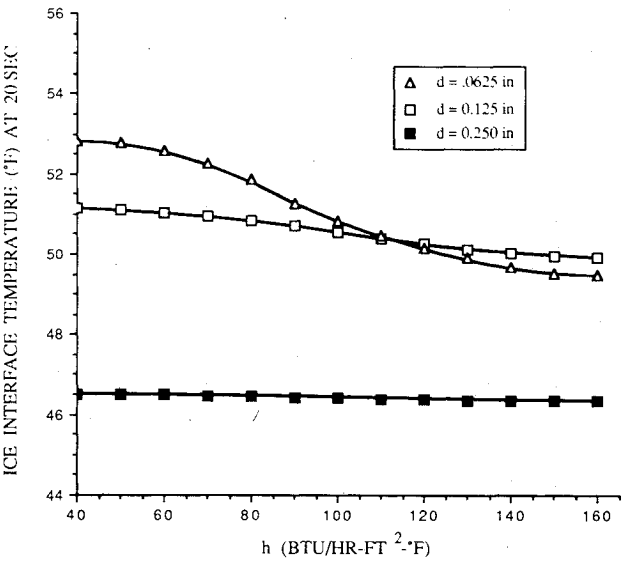

Fig. 11 Effect of a variable outer heat-transfer coefficient on ice-abrasion shield interface temperature.

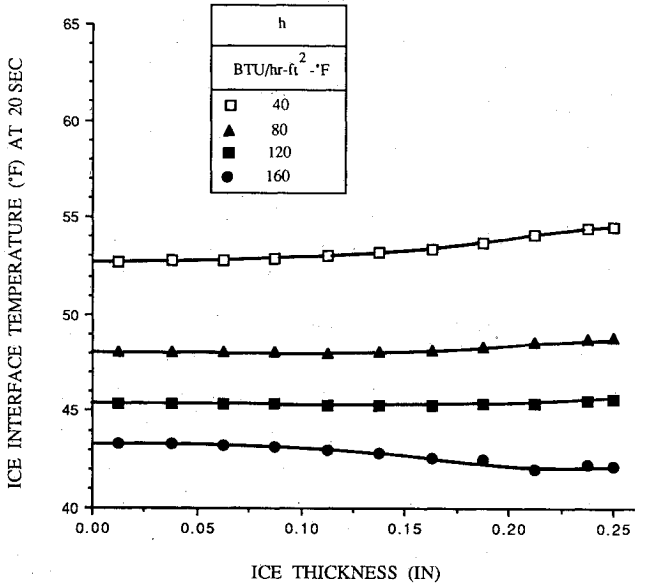

Fig. 10 Effect of variable ice thickness on ice-abrasion shield interface temperature.

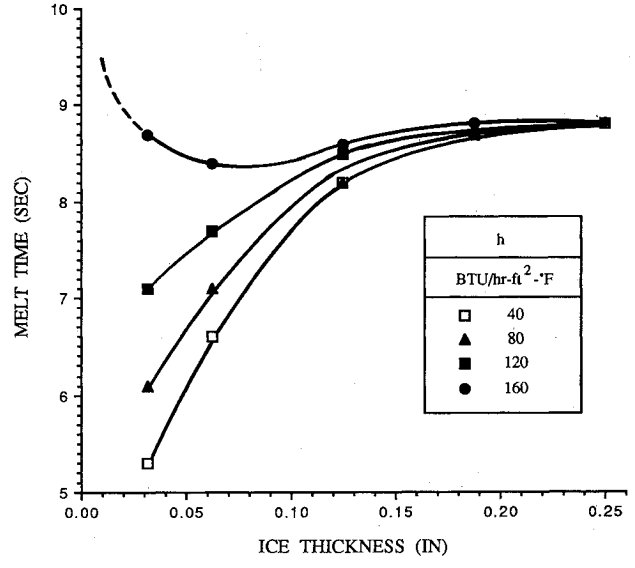

Fig. 12 Effect of ice thickness on melt times at the ice-abrasion shield interface.

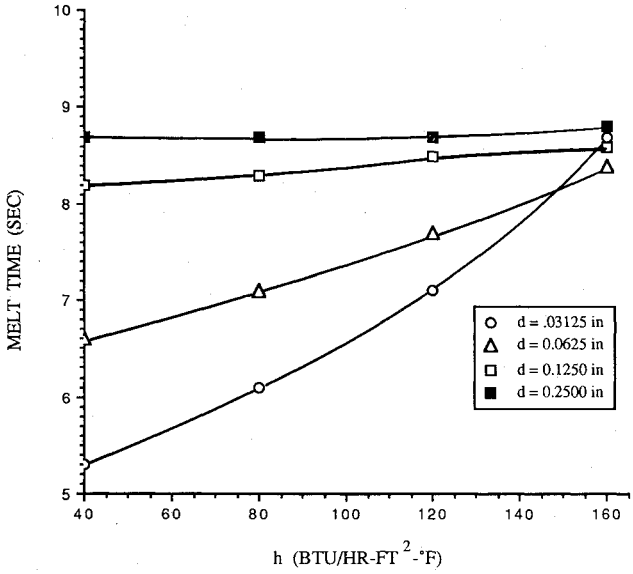

Fig. 13 Effect of outer ambient heat-transfer coefficient on melt times at the ice-abrasion shield interface.

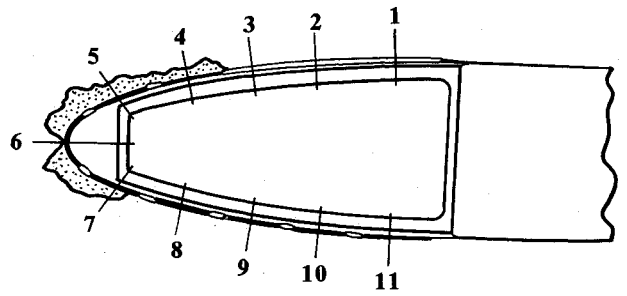

Fig. 14 Ice shape and positions of heaters around the blade.

temperature at the ice-abrasion shield interface to reach 32°F. Figure 12 shows an interesting phenomena at very low ice thicknesses. A slight increase in melt time is noticed at a heat-transfer coefficient of 160 Btu/h-ft^2-°F and an ice thickness of 0.03125 in. This point shows that for very thin ice, heat is being removed from the top surface by convection so fast that melting is taking longer to occur than it would for larger ice thicknesses. When the ice thickness becomes larger than a certain value, however, the convection surface is so distant that its effect on the abrasion shield temperature is less than the effect of the increasing ice thickness, and the melt times start to increase again. This suggests that there is a value of ice thickness at each heat-transfer coefficient for which the melt time is a minimum.

In conclusion, for the effect of a variable heat-transfer coefficient on the solution for the ice-abrasion shield interfacial temperature and for the melt times, it is felt that the heat-transfer coefficient does not need to be variable except for cases that have sections of very thin ice (<0.125 in.), or no ice at all. In addition, the absolute value of the heat-transfer coefficient does not have a strong effect on the interfacial temperature for ice thicknesses greater than 0.125 in. For the effect of variable ice thickness on the interfacial temperature, it is felt that ice thickness can be modeled as a constant if the ice thickness at every point is at least 0.125 in. It should be noted that the limiting ice thickness mentioned is dependent on the heater power density. Smaller wattages will lower this value and higher wattages will raise it. Experience with using this code reveals that if the power density is one-half the value used (15 W/in.^{2}), then the limiting ice thickness is likewise cut in half. This ratio seems to hold for other power densities as well.

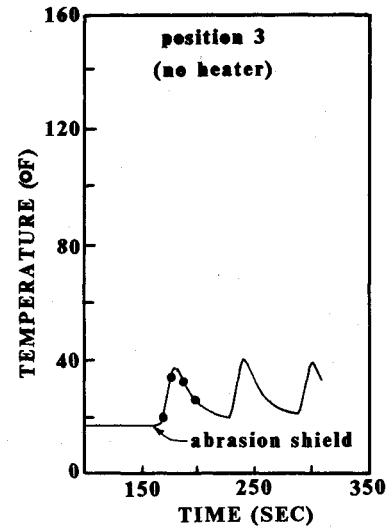

Fig. 15 Comparison of numerical model to experimental data: position 3.

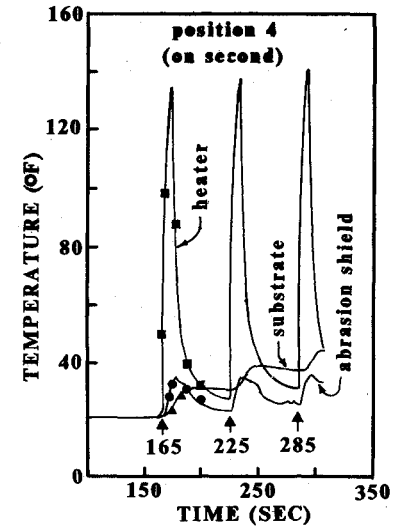

Fig. 16 Comparison of numerical model to experimental data: position 4.

Comparison with Experimental Data

The computer program was run for comparison with previously obtained experimental data.[7] The particular data set selected was a case of cyclic heating. The ice shape and thickness were known from accretion data taken at the time of the experiment. The data for the deicer pad are given in Table 3, and the various test conditions for this case are given in Table 4. Figure 14 shows the ice shape and the different positions of the heaters around the blade. Fourteen layers are modeled, which includes the ice layer. The actual blade used had different physical properties in the substrate at the stagnation point (position 6), but this cannot be modeled using this code, and the properties at this position were assumed to be the same as for the rest of the composite blade. Five heaters are modeled (positions 4–8), all of which are fired separately and have slightly different power densities. Position 3, which did not have a heater, was also modeled. A case in which the heaters are not all fired at the same time was used to show two-dimensional effects that could not be simulated before since Chao's[6] code contained only one heater. When ice is present on the blade, it is modeled as having a constant value of 0.0625 in. due to the previous discussion of the effect of ice shape on the solution. A constant heat-transfer coefficient of 70 Btu/h-ft^2-°F is assumed to be adequate for this simulation. A constant value can be assumed due to the previous discussion of the effect of heat-transfer coefficient on the solution.

Table 4 Test conditions for experimental run

Blade position	Ice thickness, in.	Heater power, W/in.^{2}	Heater on/off times, s
3	0.0	0.0	– –
4	0.0625	15.7	165/175, 225/235, 285/295
5	0.0625	15.8	165/175, 225/235, 285/295
6	0.0	15.9	165/175, 225/235, 285/295
7	0.0625	16.0	155/165, 215/225, 275/285
8	0.0	16.3	175/185, 235/245, 295/305

Deicing test commences after ice has accreted for 155 s.
Ambient temperature = 20°F.
Outer convection coefficient = 70 Btu/h-ft^2-°F.
Inner convection coefficient = 10 Btu/h-ft^2-°F.
Each heater element is 1 in. wide.
Gap between heaters is 0.061 in.

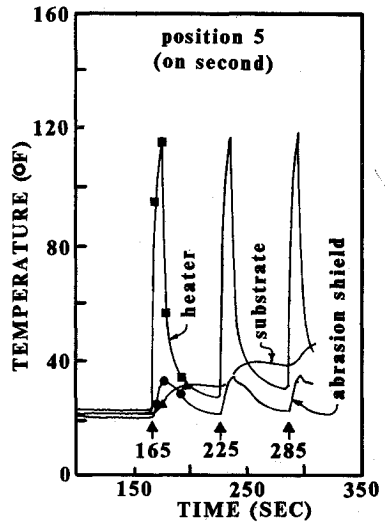

Fig. 17 Comparison of numerical model to experimental data: position 5.

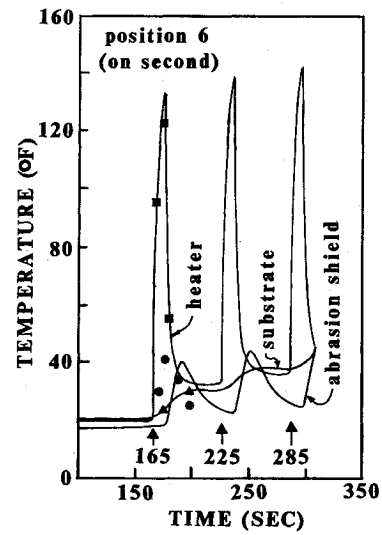

Fig. 18 Comparison of numerical model to experimental data: position 6.

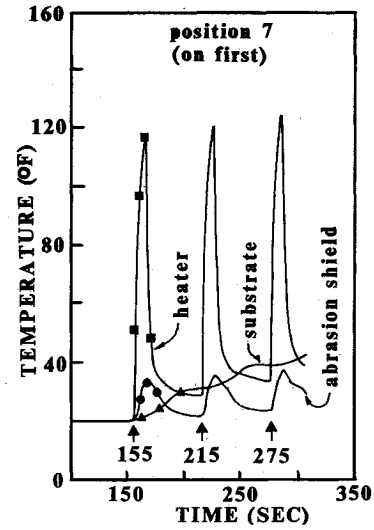

Fig. 19 Comparison of numerical model to experimental data: position 7.

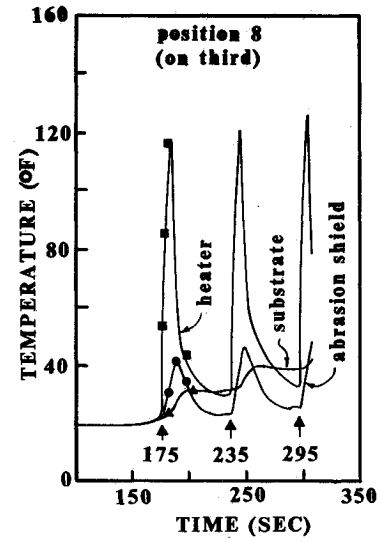

Fig. 20 Comparison of numerical model to experimental data: position 8.

Figures 15–20 plot temperature vs time at the ice-abrasion shield interface, the bottom of the heater, and the substrate for both the experimental and numerical results. The experimental results are shown as a solid line because this is the manner in which the graphics routine plots the data. The experimental data were obtained from the response of thermocouples at each position. Beyond the six positions given here, the experimental results agree with Marano's[3] one-dimensional code and therefore were not modeled with this code.

As can be seen from these figures, excellent agreement with the experimental data is obtained at positions 5, 7, and 8. At positions where ice is present, melting can be observed in both the numerical and experimental results by a slight change in slope that can be seen in the ice-abrasion shield interface temperatures. This can be seen more clearly by comparing the response at position 6, which has no ice, with the response at

position 5, which does have ice. There is a change in slope at 32°F at position 5, which indicates the ice is melting. At position 6, the abrasion shield temperature exceeds 40°F without any change in slope, which indicates that ice is not present at this position.

The response given at position 3 shows a large amount of transverse heating since a significant temperature response is noted even though this position does not contain a heater. The numerical results also show a response at this position, which agrees well with the experimental values.

The maximum heater temperatures predicted at positions 4 and 6 are lower than the experimental results despite the fact that the numerical simulation predicts the substrate and abrasion shield temperatures at these positions very well. However, the program predicts adequately the maximum heater temperatures at the other positions even though these positions have roughly the same power density as positions 4 and 6. It is believed that air gaps near the heaters at positions 4 and 6 are responsible for the difference in heater temperature. An air gap would cause the heater to reach a much higher temperature, but would not significantly change the response at other locations. This is, in fact, what is seen at these positions.

This case is clearly two-dimensional in this region, owing to the different cycles on the heaters and the absence of ice at some points on the blade. Any case that has heaters firing in different cycles should be modeled with a two-dimensional code since a one-dimensional code cannot account for the transverse heating that results from sequential firing of the heaters. Similarly, a one-dimensional code cannot handle having an ice shape such as the one present in this experimental case. However, the heater gap in the experimental case is not large enough to warrant two-dimensional analysis, as this does not create much of a two-dimensional effect. This was seen from the fact that positions 9–11 could be adequately modeled using a one-dimensional analysis even though these positions contain a heater gap, but display no other two-dimensional behavior.

Conclusions

The transient two-dimensional heat transfer in an electrothermal deicer pad has been modeled. Parametric studies were performed to investigate the effect of gap width, nodal spacing, ice thickness, and outer heat-transfer coefficient. An analysis was performed to determine when a two-dimensional rectangular model is preferred over a one-dimensional rectangular model. A comparison was also made with existing experimental data. The results of the numerical simulation were found to compare very favorably with previous numerical calculations, as well as with the experimental data.

Acknowledgments

Numerical work on electrothermal deicing has been supported by the NASA Lewis Research Center, Cleveland, Ohio, grant NAG 3-72. The authors gratefully acknowledge this continuing support and the encouragement of their work by the grant monitor, Dr. R. J. Shaw.

References

[1]Stallabrass, J. R., "Thermal Aspects of Deicer Design," Helicopter Icing Conference, Ottawa, Canada, 1972.

[2]Baliga, G., "Numerical Simulation of One-Dimensional Heat Transfer in Composite Bodies with Phase Change," M.S. Thesis, Univ. of Toledo, Toledo, OH, Aug. 1980.

[3]Marano, J. J., "Numerical Simulation of an Electrothermal Deicer Pad," M.S. Thesis, Univ. of Toledo, Toledo, OH, May 1982.

[4]Gent, R. W. and Cansdale, J. T., "One-Dimensional Treatment of Thermal Transients in Electrically Deiced Helicopter Rotor Blades," Royal Aircraft Establishment Tech. Rept. 80159, 1980.

[5]Roelke, R. J., "A Rapid Computational Procedure for the Numerical Solution of a Heat Flow Problem with Phase Change," M.S. Thesis, Univ. of Toledo, Toledo, OH, Aug. 1986.

[6]Chao, D. F., "Numerical Simulation of Two-Dimensional Heat Transfer in Composite Bodies with Application to Deicing of Aircraft Components," Ph.D. Thesis, Univ. of Toledo, Toledo, OH, Nov. 1983.

[7]Leffel, K. L., "A Numerical and Experimental Investigation of Electrothermal Aircraft Deicing," M.S. Thesis, Univ. of Toledo, Toledo, OH, Jan. 1986.

[8]Wright, W. B., "A Comparison of Numerical Methods for the Prediction of Two-Dimensional Heat Transfer in an Electrothermal Deicer Pad," M.S. Thesis, Univ. of Toledo, Toledo, OH, Feb. 1988.

[9]Masiulaniec, K. C., "A Numerical Simulation of the Full Two-Dimensional Electrothermal Deicer Pad," Ph.D. Thesis, Univ. of Toledo, Toledo, OH, June 1987.

[10]Anderson, D. A., Tannehill, J. C., and Pletcher, R. H., *Computational Fluid Dynamics and Heat Transfer,* McGraw-Hill, New York, 1984, pp. 108–138.

[11]Bonacina, C., Comini, G. Fasano, A., and Primicerio, N., "Numerical Solution of Phase Change Problems," *International Journal of Heat and Mass Transfer,* Vol. 16, Sept. 1973, pp. 1825–1832.

[12]Voller, V. and Cross, M., "Accurate Solutions of Moving Boundary Value Problems Using the Enthalpy Method," *International Journal of Heat and Mass Transfer,* Vol. 24, March 1981, pp. 545–555.

[13]Voller, V., Cross, M., and Walton, P. G., "Assessment of Weak Solution Numerical Techniques for Solving Stefan Problems," Rept. No. 172, Dept. of Mathematics and Computer Studies, Sunderland Polytechnic, UK, 1979.

[14]Atthey, D. R., "A Finite Difference Scheme for Melting Problems," *Journal of the Institute of Mathematics Applications,* Vol. 13, 1974, pp. 353–360.

[15]Schneider, G. E. and Raw, M. J., "An Implicit Solution Procedure for Finite Difference Modeling of the Stefan Problem," *AIAA Journal,* Vol. 22, Nov. 1984, pp. 1685–1690.